

IAI SPECIAL EDITION

RESEARCH ARTICLE

Molecular docking study of vemurafenib derivatives on melanoma inhibitory activity (MIA) as anti-melanoma

Fauzan Zein Muttaqin¹, Anita Pramudya Ratna Sari¹, Fransiska Kurniawan²

¹ Faculty of Pharmacy, Bhakti Kencana University, Indonesia

² School of Pharmacy, Bandung Institute of Technology, Indonesia

Keywords

Blind-docking

Melanoma

Melanoma Inhibitory Activity (MIA)

Vemurafenib

Correspondence

Fauzan Zein Muttaqin

Faculty of Pharmacy

Bhakti Kencana University

Indonesia

fauzanzein@bku.ac.id

Abstract

Background: Melanoma is one of the cancers with high mortality rates in Indonesia. The newest potential anti-melanoma target is the Melanoma Inhibitory Activity (MIA/5IXB) macromolecule, but the location of the binding pocket interaction is unknown. Vemurafenib is known to be active in vivo as against melanoma. Thus, it can be used as a lead compound. This study aimed to examine the location of the binding pocket and the interactions that occur between macromolecules and the test compounds. **Methods:** It was carried out using the blind docking method between vemurafenib and an MIA macromolecule. **Results:** The results showed that the best molecular docking was obtained in the distribution of the grid box area in the third area with a ΔG value of -7.80 kcal/mol. Docking validation results showed the value of ΔG 11.06 kcal/mol with an average value of RMSD 1.788 Å, and the amino acid residues that played a role in the interaction were MET31, TYR30, and PRO33. Targeted docking to the binding pocket results on 45 test compounds showed that the most potent compound was Compound-17 with a ΔG value of 11.31 kcal/mol with hydrophobic bond interactions on amino acid residues TYR30. This hydrophobic bond is responsible for the MIA mechanism as an inhibitor of melanoma cell metastasis in the body. It can be concluded that the binding pocket of the MIA(5IXB) macromolecule with the vemurafenib compound is at the amino acid residues MET31, TYR30, and PRO33 with the interaction of hydrogen bonds and hydrophobic bonds. Also, it was observed that T.C-17 is the most potential anti-melanoma test compound.

Introduction

Skin cancer is currently included in the diseases with high mortality rates in Indonesia. Based on research, melanoma is ranked third as deadly cancer after breast cancer and cervical cancer. Melanoma can be due to several factors, such as excessive exposure to ultraviolet radiation, an unhealthy lifestyle, and a history of genetic factors (Perera *et al.*, 2014).

Malignant melanoma can cause about a 75% higher mortality rate in skin cancer (Du *et al.*, 2013). One of the causes of malignant melanoma is a genetic mutation of the BRAF protein. Metastatic malignant melanoma due to the mutation of the BRAF protein can

be treated with BRAF inhibitors (BRAFi). BRAFi targets the BRAF V600E protein to inhibit protein cell mutation (Hernandez-Davies *et al.*, 2015). This therapy has been widely applied to melanoma patients with melanoma using vemurafenib, a first-generation BRAFi that has the potential as a very promising drug against stage 1 melanoma. However, vemurafenib showed a 63% decrease in therapeutic activity with a risk of death of up to 74% in each advanced stage melanoma patient (Madonna *et al.*, 2012).

The MIA (Melanoma Inhibitory Activity) macromolecule is known to be a potential new molecular target as anti-melanoma. MIA is an extracellular protein produced abundantly by malignant melanoma cells and plays a

crucial role in melanoma genesis, progression, and metastasis. MIA interacts directly with extracellular matrix proteins like fibronectin once it is secreted (FN). MIA induces focal cell dissociation from surrounding structures and enhances tumour cell invasion and migration by this mechanism (Yip *et al.*, 2016). Research on this new target is scarce. Therefore, the development of new drug compounds in *in-silico* studies is carried out to determine the location of the binding pocket and the type of interaction between the test compound and the target molecule (Schmidt *et al.*, 2012). In this *in-silico* study, blind-docking will be carried out to determine the location of the receptor's binding pocket with the ligand. Vemurafenib is used as a guide compound with a demonstrated activity against melanoma *in vitro* and *in vivo*. The test compounds that will be docked to the MIA macromolecule are indole alkaloid derivatives.

Based on the pharmacophore group, vemurafenib has similarities with the structure of indole alkaloid derivatives. The chemical structure of vemurafenib consists of two cyclic rings, namely benzene and a pyrrole nucleus, which are fused at the 2,3 position (Khedekar *et al.*, 2016). Indole alkaloid derivatives are expected to have better interactions and are more selective when docked to MIA macromolecules as potential new anti-melanoma drug candidates.

Methods

This research consists of several stages: preparation of the target molecule (5IXB), preparation of the lead compound and the test compounds, determination of the binding pocket, validation of docking, targeted docking to predict the affinity of the test compound to the target molecule.

MIA 3-dimensional structure file downloaded from [rscb](https://www.rcsb.org/) website with PDB ID: 5IXB, in *.pdb file format (Figure 1).

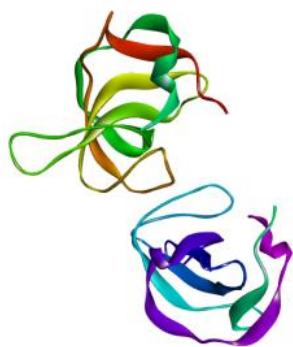


Figure 1: 3-D structure of MIA (5IXB)

Water molecules and other residues on macromolecules were removed using the Discovery Studio 2016 software. Then, the polar hydrogen was added, and the charge on the macromolecule was calculated. Optimisation of the geometric structure of the lead compound (vemurafenib) and the test compounds (indole alkaloid derivatives) was carried out using Gaussian 09 software with the Density Functional Theory (DFT) optimisation method; basis set of 6-31 G. Optimisation was continued by adjusting the partial charge of the lead and test compounds in AutoDock Tools v.4.2.3 software.

The search for binding pockets between the target molecule and the lead compound employed a docking simulation using AutoDock Tools v.4.2.3 to predict the position of the complex between the lead compound and the MIA macromolecule so that it can be continued with docking validation to ensure the exact location of the interaction. Docking validation meets the requirements if the average value of RMSD < 2Å and the amino acid residue that plays a role in the bonding interaction is known (Hevener *et al.*, 2009). Then the targeted docking of the test compound to the MIA macromolecule was carried out on 45 indole alkaloid derivatives to determine the lowest free binding energy and amino acid residues responsible for the bond formation with the test compound.

Result

The initial step in searching for the binding pocket, where the macromolecule interacts with the ligand (Table I) using Autodock Tools v.4.2.3 software was to divide the macromolecular grid box area into four parts, with the aim that the grid box covers all macromolecular areas, followed by docking of the lead compound toward the macromolecule in each area (Table II and Figure 2).

Table I: Docking Area Division on MIA Macromolecule

Grid box area	Grid box size (x,y,z)	Grid box coordinate			ΔG (kcal/mol)
		x	y	z	
1	126,58,92	-5.844	2.327	20.400	-6.41
2	126,58,86	-6.478	-16.809	17.719	-6.82
3	100,72,84	4.126	-4.772	46.617	-7.80
4	108,66,106	1.388	-30.000	46.906	-6.74

Ligand pose extraction was carried out five times by reducing the grid box area with GA medium mode, run: 100, and setting the grid box position at the centre on the ligand during the docking process (Table III). Docking validation was carried out five times on the grid box extracted from the best ligand pose (Table IV). Then targeted docking of 45 indole alkaloid derivatives was carried out using the grid box parameter that had been validated (Table V and Figure 3).

Table II: The result of the interaction of MIA macromolecular amino acid residues with the lead compound

Grid box area	ΔG (kcal/mol)	Amino acid residue	Lead compound	Interaction type	Grid box area	ΔG (kcal/mol)	Amino acid residue	Lead compound	Interaction type
1	-6.41	A:LYS 53	O 6	Hydrogen bond	3	-7.80	A:GLN 28	O 7	Hydrogen bond
		A:LYS 53	O 7	Hydrogen bond			B:TYR 30	F 4	Hydrogen bond
		A:LYS 53	O 6	Hydrogen bond			A:TYR 30	Aromatic	Hydrophobic bond
		A:GLY 54	O 7	Hydrogen bond			B:TYR 30	Aromatic	Hydrophobic bond
		A:TRP 60	N 10	Hydrogen bond			B: ILE 83	Aromatic	Hydrophobic bond
		A:LYS 94	O 5	Hydrogen bond			A:TYR 30	Aromatic	Hydrophobic bond
		A:ARG 57	H 41	Hydrogen bond			B:TYR 30	Aromatic	Hydrophobic bond
2	-6.82	1. A:LYS 10	O 7	Hydrogen bond	4	-6.74	B:ARG 55	F 3	Hydrogen bond
		2. A:LEU 76	Aromatic	Hydrophobic bond			B:ARG 55	O 5	Hydrogen bond
		3. A:LEU 76	Aromatic	Hydrophobic bond			B:ARG 55	F 3	Hydrogen bond
		4. A:TYR 78	Aromatic	Hydrophobic bond			B:ARG 55	F 3	Hydrogen bond
		5. A:TYR 78	Aromatic	Hydrophobic bond			B:ARG 55	O 5	Hydrogen bond
							B:ARG 55	F 3	Hydrogen bond
							B:ARG 55	O 5	Hydrogen bond
							B:PRO 4	H 41	Hydrogen bond
							B:LEU 6	Aromatic	Hydrophobic bond

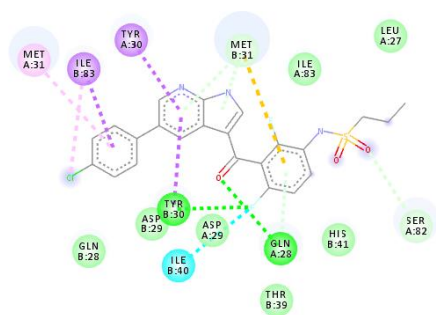


Figure 2: 2-D visualization of Vemurafenib docking toward MIA macromolecule in the 3rd grid box area

Table III: Ligand pose extraction at the 3rd grid box area

Extraction step	Grid box size (x,y,z)	Grid box coordinate			Run	ΔG (kcal/mol)
		x	y	z		
1	90,60,70	-0.39	-8.89	34.43	78	-10.93
2	80,50,64	-5.12	-12.21	33.06	40	-10.99
3	70,48,54	-4.99	-12.14	32.99	89	-11.02
4	46,52,50	-4.96	-12.41	32.97	38	-11.09
5	44,42,34	-4.97	-12.38	32.91	79	-11.07

Table IV: Docking validation result

No	ΔG (kcal/mol)	RMSD	Amino acid residue	Lead compound	Interaction type	No	ΔG (kcal/mol)	RMSD	Amino acid residue	Lead compound	Interaction type
1	-11.10	1.707	MET 31	N 10	Hydrogen bond	4	-11.08	1.779	MET 31	N 10	Hydrogen bond
			A:TYR 30	Aromatic	Hydrophobic bond				A:TYR 30	Aromatic	Hydrophobic bond
			B:TYR 30	Aromatic	Hydrophobic bond				B:TYR 30	Aromatic	Hydrophobic bond
			A:TYR 30	Aromatic	Hydrophobic bond				A:TYR 30	Aromatic	Hydrophobic bond
			A:PRO 33	Aromatic	Hydrophobic bond				A:PRO 33	Aromatic	Hydrophobic bond
2	-11.13	1.803	MET 31	N 10	Hydrogen bond	5	-11.10	1.806	MET 31	N 10	Hydrogen bond
			A:TYR 30	Aromatic	Hydrophobic bond				A:TYR 30	Aromatic	Hydrophobic bond
			B:TYR 30	Aromatic	Hydrophobic bond				B:TYR 30	Aromatic	Hydrophobic bond
			A:TYR 30	Aromatic	Hydrophobic				A:TYR 30	Aromatic	Hydrophobic

No	ΔG (kcal/mol)	RMSD	Amino acid residue	Lead compound	Interaction type	No	ΔG (kcal/mol)	RMSD	Amino acid residue	Lead compound	Interaction type
					bond						bond
			A:PRO 33	Aromatic	Hydrophobic bond				A:PRO 33	Aromatic	Hydrophobic bond
			MET 31	N 10	Hydrogen bond						
			A:TYR 30	Aromatic	Hydrophobic bond						
3	-11.12	1.846	B:TYR 30	Aromatic	Hydrophobic bond						
			A:TYR 30	Aromatic	Hydrophobic bond						
			A:PRO 33	Aromatic	Hydrophobic bond						

Table V: Targeted docking result of alkaloid indole derivatives

Test compound	ΔG (kcal/ mol)	Ki	Amino acid residue	Interaction type	Test compound	ΔG (kcal/ mol)	Ki	Amino acid residue	Interaction type
T.C-15	-8.85	323.99 nM	B:TYR 30	Hydrophobic bond	T.C-21	-5.30	131.38 μ M	A:MET 31-O	Hydrogen bond
			B:TYR 30	Hydrophobic bond				A:TYR 30	Hydrophobic bond
T.C-16	-6.96	7.86 μ M	B:TYR 30	Hydrophobic bond	T.C-22	-8.79	360.20 nM	A:TYR 30	Hydrophobic bond
			B:TYR 30	Hydrophobic bond				B:TYR 30	Hydrophobic bond
T.C-17	-11.31	5.16 nM	A:TYR 30	Hydrophobic bond	T.C-23	-7.46	3.38 μ M	A:MET 31-H	Hydrogen bond
			B:TYR 30	Hydrophobic bond				A:TYR 30	Hydrophobic bond
			B:TYR 30	Hydrophobic bond	T.C-24	-10.36	25.43 nM	B:TYR30	Hydrophobic bond
T.C-18	-8.02	1.31 μ M	None	None	T.C-25	-9.54	100.97 nM	A:TYR 30	Hydrophobic bond
T.C-19	-9.24	168.54 nM	None	None	T.C-26	-8.82	341.31 nM	B:TYR 30	Hydrophobic bond
T.C-20	-7.38	3.86 μ M	A:MET 31-O	Hydrogen bond				B:TYR 30	Hydrophobic bond
			A:MET 31-O	Hydrogen bond					
			B:MET 31-H	Hydrogen bond					

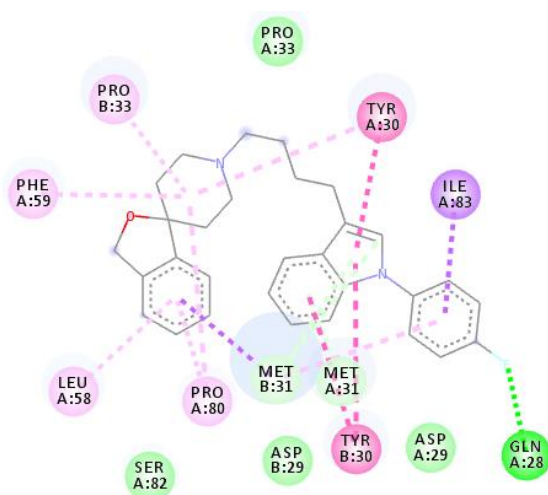


Figure 3: 2-D visualization of T.C-17 docking toward MIA macromolecule

Discussion

The most negative free binding energy (ΔG) was found in the third grid box area (Table I). This value indicates that the predicted ligand pose has a good interaction. Visualisation of the docking results in Figure 2 shows that the interaction between the macromolecule and the lead compound in the grid box 3 area is relatively stable with the formation of hydrophobic and hydrogen bonds.

As shown in Table II, the third grid box area has the most negative ΔG , which is -7.80 kcal/mol. The visualisation results showed that the interactions in the MIA macromolecular complex with the lead compound were two hydrogen bonds and five hydrophobic bonds.

Hydrogen bonds are reversible, where the bonds can be broken and reconnected with other groups. Thus, a compound with hydrogen bonds can be easily metabolised. Hydrogen bonds are essential in drug

compounds' interactions with target molecules (Varma *et al.*, 2010).

The hydrophobic bonds in the MIA interaction with vemurafenib occur because the amino acid residues Tyrosine 30 and Isoleucine 83 interact with the aromatic compounds on the lead compound.

These data indicate that the vemurafenib interaction in the third grid box area was chosen as a potential anti-melanoma agent targeting MIA macromolecules.

The best ligand pose extraction results (Table III) show that the correct grid box size is 44,42,34 (x,y,z) with grid box coordinates 4.97, 12.376, 32.905 (x,y,z), which is then used for the docking validation stage, resulting in the free binding energy of 11.06 kcal/mol and a qualified RMSD of 1.788 Å, as shown in Table IV.

The results of targeted docking of 45 indole alkaloid derivatives in Table V show that the test compound SU-17 is the most potential candidate compound as an anti-melanoma agent that interacts with MIA macromolecules with the lowest free binding energy and inhibition constant values of -11.31 kcal/mol and 5.16 nM, respectively.

The K_i value indicates the ability of a compound to inhibit the activity of its target molecule. The smaller the K_i value, the better the inhibition. This result shows that a small concentration of the test compound can provide an excellent inhibitory effect.

Visualisation of the interaction of the test compound T.C-17 with MIA macromolecules in Figure 3 shows that the amino acid residue that plays a role in the interaction is Tyrosine 30 (TYR 30) with a hydrophobic bond interaction type.

When the TYR 30 amino acid residue binds to the aromatic group of the compound T.C-17, the MIA macromolecule is inhibited, which results in cancer cells not metastasising to other tissues and organs. The most dangerous phase of this malignant melanoma is metastases, where the cancer cells invade other vital body tissues and organs. Therefore, this MIA agent would be very effective if used as anti-melanoma therapy at that phase appropriately.

Conclusion

The location of the binding pocket of the MIA(5IXB) macromolecule with the compound vemurafenib was obtained at the amino acid residue MET31, TYR30, and PRO33 with the interaction of hydrogen bonds

and hydrophobic bonds. The test compound T.C-17 showed to be a potential indole alkaloid derivative anti-melanoma drug candidate.

References

- Du, J., Lu, X., Long, Z., Zhang, Z., Zhu, X., Yang, Y., & Xu, J. (2013). *n Vitro and in Vivo Anticancer Activity of Aconitine on Melanoma Cell Line B16. International Journal of Molecular Sciences*, **18**(1), 757–767. <https://doi.org/10.3390/molecules18010757>
- Hernandez-Davies, J. E., Tran, T. Q., Reid, M. A., Rosales, K. R., Lowman, X. H., Pan, M., Moriceau, G., Yang, Y., Wu, J., Lo, R. S., & Kong, M. (2015). Vemurafenib resistance reprograms melanoma cells towards glutamine dependence. *Journal of Translational Medicine*, **13**(1). <https://doi.org/10.1186/s12967-015-0581-2>
- Hevener, K. E., Zhao, W., Ball, D. M., Babaoglu, K., Qi, J., White, S. W., & Lee, R. E. (2009). Validation of molecular docking programs for virtual screening against dihydropteroate synthase. *Journal of Chemical Information and Modeling*, **49**(2), 444–460. <https://doi.org/10.1021/ci800293n>
- Khedekar, P., Kerzare, D. R., Khedekar, P. B., & Kerzarea, D. R. (2016). Indole Derivatives acting on Central Nervous System-Review. *Journal of Pharmaceutical sciences and bioscientific research*. 2016, **6**(1), 144–156. www.jpsbr.org
- Madonna, G., Ullman, C. D., Gentilcore, G., Palmieri, G., & Ascierto, P. A. (2012). NF- κ B as potential target in the treatment of melanoma. In *Journal of Translational Medicine* (Vol. 10, Issue 1). <https://doi.org/10.1186/1479-5876-10-53>
- Perera, E., Gnaneswaran, N., Jennens, R., & Sinclair, R. (2014). Malignant melanoma. In *Healthcare (Switzerland)* (Vol. 2, Issue 1, pp. 1–19). MDPI. <https://doi.org/10.3390/healthcare2010001>
- Schmidt, J., Riechers, A., Stoll, R., Amann, T., Fink, F., Spruss, T., Gronwald, W., König, B., Hellerbrand, C., & Bosserhoff, A. K. (2012). Targeting melanoma metastasis and immunosuppression with a new mode of melanoma inhibitory activity (MIA) protein inhibition. *Public Library of Science*, **7**(5). <https://doi.org/10.1371/journal.pone.0037941>
- Varma, A. K., Patil, R., Das, S., Stanley, A., Yadav, L., & Sudhakar, A. (2010). Optimized hydrophobic interactions and hydrogen bonding at the target-ligand interface leads the pathways of Drug-Designing. *Public Library of Science*, **5**(8). <https://doi.org/10.1371/journal.pone.0012029>
- Yip, K. T., Zhong, X. Y., Seibel, N., Pütz, S., Autzen, J., Gasper, R., Hofmann, E., Scherckenbeck, J., & Stoll, R. (2016). Small Molecules Antagonise the MIA-Fibronectin Interaction in Malignant Melanoma. *Scientific Reports*, **6**. <https://doi.org/10.1038/srep25119>